Surface induced crystallographic order in sexiphenyl thin films

2008 J. Phys.: Condens. Matter 20 184009

(http://iopscience.iop.org/0953-8984/20/18/184009)

IOP PUBLISHING JOURNAL OF PHYSICS: CONDENSED MATTER

J. Phys.: Condens. Matter **20** (2008) 184009 (10pp) doi:10.1088/0953-8984/20/18/184009

Surface induced crystallographic order in sexiphenyl thin films

R Resel

Institute of Solid State Physics, Graz University of Technology, Austria

E-mail: roland.resel@tugraz.at

Received 4 September 2007, in final form 24 October 2007
Published 17 April 2008
Online at stacks.iop.org/JPhysCM/20/184009

Abstract

The crystallographic order in sexiphenyl thin films on dielectric surfaces (like thermally oxidized silicon, KCl(100), TiO_2(110) mica (001)) and on metallic surfaces (like Au(111), Al(111)) are summarized. The combination of the surface science studies considering the first molecular layers on the substrate surfaces with crystallographic studies on sexiphenyl films reveals the influence of the first molecular layers on the thin-film structure. The interaction strength of the molecules with the substrate has a large influence on the preferred orientation of the crystallites relative to the substrate surface. In the case of metallic surfaces, the orientation of the molecules at the first monolayer determines the alignment of the crystallites in the thin film. In the case of dielectric surfaces, other types of preferred crystal orientations are observed, which is connected with the increasing importance of the intermolecular interaction strength in the first monolayers. Generally, it is observed that the bulk crystal structure is already present in thin films with a nominal thickness slightly larger than the monolayer thickness. The orientation and alignment of the initial crystal clusters at the surface determine the layer growth. The thin films show specific morphologies: depending on the orientation of the molecules relative to the substrate surface, either terraced islands or needle-like structures appear. The crystallite size parallel to the surface varies in a range from nanometres up to several tens of microns, depending on the type of substrate and the thin-film growth conditions. In the case of terraced islands, the crystallite size perpendicular to the surface is comparable with the nominal film thickness.

(Some figures in this article are in colour only in the electronic version)

1. The application relevance of the molecule sexiphenyl

The molecule sexiphenyl (frequently also denoted as hexaphenyl) is a wide-gap organic semiconductor with an energy gap of around 3.1 eV [1, 2]. The outstanding properties of sexiphenyl (in the following text, abbreviated by p-6P) are the photoluminescence in the blue visible range with high photoluminescence quantum yield, together with excellent chemical stability [3, 4]. Light-emitting devices based on p-6P show blue electroluminescence [5, 6]; light emitting devices for polarized light emission were built [7] and the possible use of p-6P in large-area flat-panel displays was demonstrated [8]. Until now, p-6P—as a member of the family of oligophenylene molecules—plays a role in current display technology based on organic electroluminescence [9]. The potential of the molecule in other optical applications is also demonstrated for optical waveguides [10–12], as a laser dye [13, 14], in nonlinear optics [15] and in laser applications [16, 17].

The optical properties of p-6P molecules as well as the electronic properties of p-6P crystallites are highly anisotropic [18, 19]. It is shown for light-emitting devices that a well-chosen thin-film geometry can enhance the device performance considerably [20]. Such examples reveal that the orientation and alignment of the molecules within thin films are of large importance. The aim of this paper is to summarize the current knowledge of the crystallographic order in p-6P thin films. In the last few years huge progress has been made in the knowledge of p-6P thin-film growth, and these developments in particular are considered. The correlation between the crystallographic order and the thin-film morphology is presented and, additionally, the role of the first molecular monolayer for thin-film formation is discussed for some specific cases. The thin-film properties of p-6P

Table 1. The experimentally observed preferred orientations of sexiphenyl crystals on various substrates are listed. The type of film preparation methods like physical vapour deposition (PVD), hot-wall epitaxy (HWE) and molecular beam epitaxy (MBE), the type of substrate, the substrate temperature during the thin film deposition, and the type of crystal orientation (minor fractions given in brackets) are given, together with the corresponding references.

Deposition method	Substrate	Substrate temperature	Crystal orientations	References
PVD	SiO_x	77 K[a]	B C (random)	[51]
HWE	SiO_x	RT	B C (A)	[38, 39, 98]
HWE	SiO_x	>400 K	S S′ of γ-phase	[36, 37, 97]
PVD	Rubbed surfaces	RT	A (B C D)	[55, 76, 78]
HWE	KCl(100)	363 K	A B C S	[50, 54, 83–85]
HWE	KCl(100)	>400 K	A S (B C)	[53]
MBE	TiO_2(110)	RT	A	[27, 66]
MBE	TiO_2(110)	370 K	S	[52]
HWE	Mica (001)	293 K	B (C S)	[100]
HWE	Mica (001)	393 K	B (C)	[87, 89, 99]
HWE	Mica (001)	430 K	B C	[89, 100]
MBE	Au(111)	77 K[a]	Random	[26]
MBE	Au(111)	300 K, 330 K	D	[91]
MBE	Au(111)	430 K	D (S)	[26, 91]
MBE	Al(111)	RT	D	[90]
MBE	Al(111)	423 K	D S	[90]

[a] Grown at 77K and annealed at room temperature (RT).

are, besides copper-phthalocyanine, PTCDA, sexithiophene and pentacene, the best-studied thin-film system of polynuclear aromatic molecules.

2. Thin-film preparation and characterization

Since p-6P is insoluble in any known solvent, only vapour deposition methods can be used for thin-film preparation. The type of substrate, as well as the substrate surface purity prior to thin-film deposition, are important parameters which influence the thin-film growth. For example, it has been shown that a sub-monolayer coverage of carbon on a Au(111) surface changes totally the crystallographic order and the thin-film morphology of quaterphenyl thin films [21]. Also, an oxygen termination of an Al(111) surface causes a change in the molecular orientation of p-6P compared with the pure Al(111) surface [22]. The p-6P thin films considered in this review are prepared by either molecular beam epitaxy (MBE) under ultra-high-vacuum conditions [23, 24] or in high vacuum by physical vapour deposition (PVD) or by hot-wall epitaxy (HWE) approaching thermodynamical equilibrium growth conditions [25]. The thin-film systems that were considered are listed in table 1.

When p-6P is deposited at growth temperatures close to liquid nitrogen temperatures an amorphous state of the thin film is observed. Annealing of amorphous films at room temperature results in polycrystalline films with random distributed crystal orientations or with a weak texture. Thin-film deposition on substrates kept at room temperature yield highly crystalline films. Above a substrate temperature of 500 K, no thin film (except the first monolayer in some cases) can be deposited [26].

The properties of the molecules in the first monolayer on the substrate are investigated by scanning tunnelling microscopy (STM), by thermal desorption spectroscopy (TDS), by photoelectron spectroscopy (UPS, ARUPS, XPS), by low-energy electron diffraction (LEED) and by grazing incidence x-ray surface diffraction. Several monolayer-sensitive techniques are limited only to conductive (metallic) surfaces, since most of the techniques are difficult to apply to non-conducting (dielectric) surfaces.

The crystallographic studies were performed by x-ray diffraction (XRD) in combination with transmission electron microscopy and diffraction (TEM/TED). The XRD studies are used to get an integral characterization of the whole thin film with high resolution in the reciprocal space. Films of nominal thicknesses larger than 30 nm are investigated by using XRD laboratory equipment. Methods like specular diffraction, in-plane and out-of-plane rocking curves, reciprocal space maps and pole figures are performed. Films with a thickness of smaller that 30 nm are investigated by grazing incidence diffraction using synchrotron radiation. Based on the XRD results, spatially resolved investigations were performed by TEM/TED; methods like selected area diffraction, dark-field imaging and high-resolution microscopy are applied. Details of the applied diffraction methods can be found elsewhere [27]. The morphologies of the thin films are investigated mainly by atomic force microscopy (AFM) but also by scanning electron microscopy (SEM).

3. Crystal structure properties of sexiphenyl

Sexiphenyl ($C_{36}H_{26}$) is an aromatic molecule consisting of six phenyl rings arranged along one line. This axis is denoted as the long molecular axis. The equilibrium conformation of an individual molecule shows a twist angle between neighbouring phenyl rings of more than 40° [28]. However, in the crystalline state (under ambient conditions) all phenyl rings are arranged in one plane (the so-called aromatic plane). However, thermally activated oscillations of the phenyl rings around the long molecular axis (called librations) and randomly distributed tilts of neighbouring phenyl rings appear in the

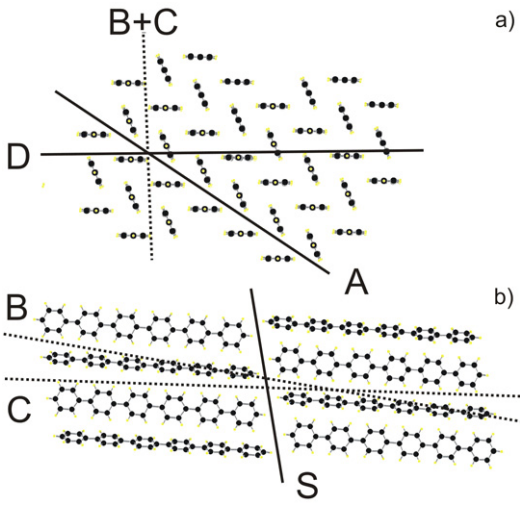

Figure 1. The molecular arrangement of the sexiphenyl molecules within the β-structure; the view along the molecular axes of a single herringbone layer (a) and the arrangement of two herringbone layers besides each other (b). Crystallographic planes which are in thin films parallel to the substrate surface are represented by lines. The plane $(20\bar{3})$ corresponds to A, $(11\bar{1})$ to B, $(11\bar{2})$ to C, $(21\bar{3})$ to D and (001) to S.

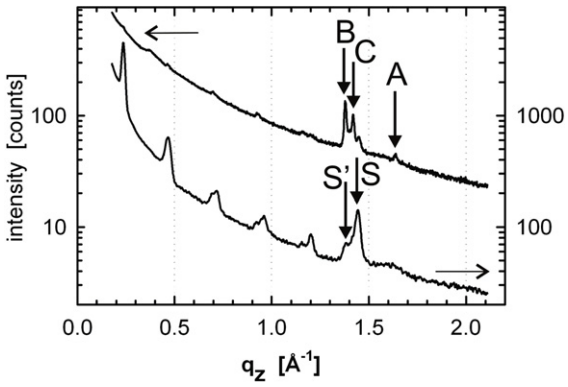

Figure 2. Specular x-ray diffraction of two sexiphenyl thin films prepared on thermally oxidized silicon at substrate temperatures of 300 K (above) and 433 K (below). The preferred orientations of the crystallites with β-structure are marked by A, B, C and S; S′ denotes another preferred orientation with the γ-structure of sexiphenyl.

crystalline state, so that neighbouring phenyl rings are slightly tilted out of the aromatic plane of less than 10° [28, 29].

P-6P crystallizes in the monoclinic space group $P2_1/c$ with the lattice constants $a = 8.091$ Å, $b = 5.568$ Å, $c = 26.24$ Å and $\beta = 98.17°$ [28, 30]. The crystal structure is classified as a layered herringbone structure, as is typical for all aromatic molecules with a rigid rod-like structure [31, 32]. Figure 1 shows the arrangement of the molecules within the crystal structure. Two herringbone layers are drawn in figure 1(b), where four molecules are plotted per layer. The arrangement of the molecules within one single herringbone layer is drawn in figure 1(a); the molecules are projected along their long molecular axes. The side tilting of neighbouring aromatic planes is a consequence of quadrupolar interaction between the phenyl rings of neighbouring molecules [33, 34]. Theoretical calculations reveal that the plane between two herringbone layers which is the (001) net plane (marked as S in figure 1(b)) shows the smallest surface energy of all lattice planes of the p-6P crystal structure [35]. As a consequence, a plate-like crystal morphology is formed from p-6P crystals [28].

Further crystallographic important lattice planes—denoted with A, B, C and D—are drawn in figure 1. These planes represent crystallographic planes which are observed in thin films parallel to the substrate surface. Crystallites with orientations A, B, C and D show the $(20\bar{3})$, $(11\bar{1})$, $(11\bar{2})$ and $(21\bar{3})$ planes parallel to the substrate surface, respectively. Please note that, in case of the crystal orientations A, B, C and D, the long axes of the molecules are approximately parallel to the substrate surface. Crystals with orientation S are oriented with the (001) net plane (the plane of the herringbone layers) parallel to the substrate surface. Please note that crystallites with orientation S arise from molecules which are standing approximately upright relative to the substrate.

The molecule p-6P has only a weak tendency to form polymorph crystal structures. It is known that, at around 110 K, a phase transition appear [28]. This phase transition is accompanied by a change of the molecular conformation from an average flat molecule to a molecule with defined twist angles of neighbouring phenyl rings in the crystalline state. Moreover, one additional crystal structure is observed in thin films which represents a surface-induced polymorph structure, denoted as γ-phase [36, 37]. All three known polymorph structures are layered herringbone structures.

4. Preferred orientation of sexiphenyl crystals

P-6P thin films grown on isotropic substrates (glass surfaces, native oxide single crystalline surfaces or thermally oxidized silicon) show a pronounced preferred orientation of the crystallites, which means that one specific crystallographic plane is parallel to the substrate surface. However, due to the isotropic nature of the substrate surface, no in-plane alignment of the crystallites is present. Such a type of thin film can be termed a two-dimensional powder. Figure 2 shows two x-ray diffraction patterns (specular scans) of two p-6P thin films with a thickness of about 100 nm on an oxidized silicon surface. The films are prepared at different substrate temperatures and, generally, it is observed that at low substrate temperature (and high deposition rates) the crystal orientations A, B, and C are present [38, 39]. In the case of enhanced substrate temperatures (and low deposition rates) a $00L$ peak series of the interplanar distance of 26.0 Å is present, which is typical for the orientation S [38]. Additionally, another polymorph of p-6P is formed which shows a similar peak series arising from an interplanar distance of 27.2 Å [36, 37]. In figure 2 the 006 reflection of the p-6P bulk structure and of the polymorph structure are marked by arrows denoted with S and S′, respectively. It is observed that, especially at elevated substrate temperatures, surface polymorph phases are formed that are different to the equilibrium bulk structure; it seems that the surface of the substrate induces another crystal structure to p-6P. Such surface-induced polymorph structures are also

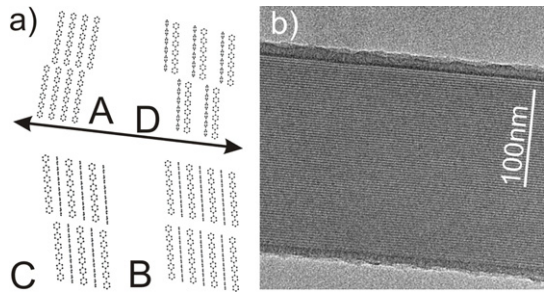

Figure 3. The four arrangements of the sexiphenyl molecules within individual sexiphenyl needles; two herringbone layers are drawn for each case (a). High-resolution transmission electron microscopy of a sexiphenyl needle grown on KCl(100); the individual herringbone layers are visible (b).

found in thin films of other rigid rod conjugated molecules like pentacene or sexithiophene [40–42].

The preferred orientation of the crystallites is accompanied by typical morphologies. Thin films with crystal orientation S typically show terraces (or terraced islands) as their thin-film morphology [43–45], while crystal orientations A, B, C, and to some extend also D, show typical needle-like morphology [46–49]. In both cases the low attachment energy of the molecules to the (001) plane and the comparable high attachment energy of the molecules to attach themselves to the herringbone layer is responsible for the crystal morphology. Up-right standing molecules induce crystal growth in two lateral dimensions with stacking of herringbone layers above each other parallel to the substrate surface. Molecules that are lying induce growth in one lateral dimension with (001) as facets, resulting in a needle-like morphology. Figure 3 shows the alignment of the p-6P molecules within a singe needle. In figure 3(a) the double arrow gives the needle axis and the orientation of the molecules is given for the four responsible types of crystal orientation. The molecules show, for the four crystal orientations, individual tilt angles relative to the needle axis. Only for orientation A are the molecules absolutely perpendicular to the needle axis; for orientation B, C and D tilt angles of 75°, 76° and 80° appear, respectively. Figure 3(b) shows a high-resolution transmission electron microscopy image of a single p-6P needle grown on KCl(100). The individual herringbone layers with an interplanar distance of 2.6 nm are clearly visible. No crystal defect is visible in the whole picture, which reveals that the p-6P needle that is shown represents a single crystal [50].

5. Crystallites with up-right standing orientation of molecules

There are two different growth conditions that induce crystallites with up-right standing molecules: (i) enhanced substrate temperature during film deposition [38, 51–53] and surface contamination [21, 22]. The presence of up-right standing p-6P molecules in the early growth stage is observed on isotropic substrates, but also on TiO_2(110), mica (001) (compare table 1) [43, 52]. On isotropic surfaces the first few layers show a layer-by-layer growth; at a nominal thickness

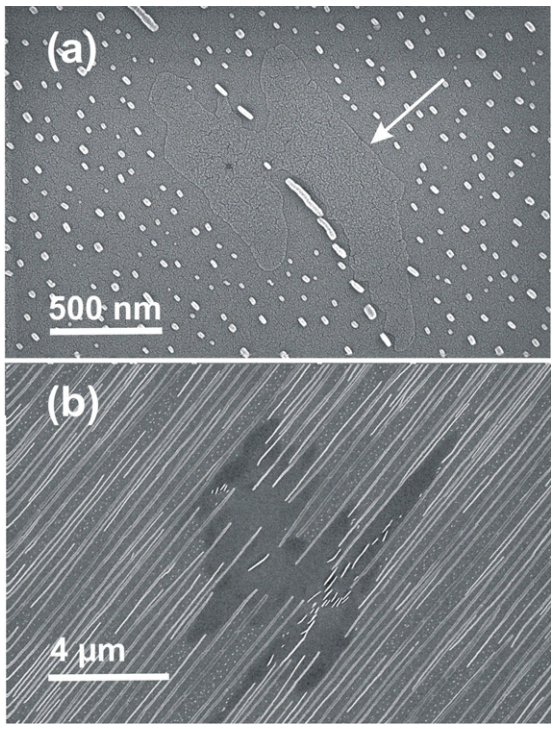

Figure 4. Scanning electron microscopy images of a sexiphenyl thin film on mica (001) grown at 293 K for 2 min (a) and for 20 min (b). The arrow denotes the border of an extended sexiphenyl terrace (a).

of two layers the growth of terraced islands starts [38]. At larger film thickness these islands grow together by static coalescence.

Figure 4 shows two microscopy images of p-6P thin films grown on a mica (001) surface. The first image is taken in the early growth stage, where an extended terrace besides elongated islands is visible. During the thin-film growth the terrace hinders the needle formation, so that in the advanced growth state the p-6P needles are disturbed by the initial growth defects of p-6P terraces.

There also exist several examples where crystallites with up-right standing p-6P molecules do not appear in the initial growth stage, but appear in the advanced growth stage, as observed on KCl(100) and Au(111), [26, 54]. In both cases crystallites with molecules that are lying down are formed initially. Therefore, the formation of crystals with orientation S is identified as a secondary growth process. The basic formation of crystals with orientation S seems to be a two-step process: (i) the development of crystalline clusters with lying molecules and (ii) a re-orientation of the molecular clusters from a lying crystal orientation to orientation S. Obviously—as experimentally observed—surface contamination and activation by temperature plays an important role in the formation of crystal orientation S.

An example of an epitaxially grown p-6P thin film is the growth on oxygen-reconstructed TiO_2(110) at elevated substrate temperatures [52]. The crystal morphology shows terraced islands with extended terrace sizes up to 100 μm [45]. P-6P crystals grow with orientation S already in the first monolayers and, interestingly, the monolayer already shows

the bulk crystal structure. No surface-induced polymorph structure is observed. The epitaxial order in the system is induced by the strong surface corrugation of the substrate, and the extremely small in-plane mosaicity of less than 0.4° is outstanding. The lateral crystal size (parallel to the substrate surface) is anisotropic, with typical dimensions of 30 and 300 nm [52].

X-ray diffraction line profile analysis on thin films with crystal orientation S was performed to get information about crystal size and microstrain within the crystals. It was found that the peak broadening is caused predominantly by size contributions, so that microstrain is negligible in p-6P and quaterphenyl thin films [55, 56]. The crystal size—determined perpendicular to the substrate surface—is comparable to the nominal film thickness.

6. Monolayer formation on crystal surfaces

The formation of the first p-6P monolayer on inorganic surfaces is studied for metallic and dielectric surfaces. In the case of metallic surfaces, detailed studies are performed on Au(111) [57, 58], which allows a direct comparison with the monolayer properties of quaterphenyl [59, 60]; further results are obtained for Ni(110) [61], Al(111) [62, 63], Cu(110) and Cu(110)-(2 × 1)O [64, 65]. Dielectric surfaces are less studied in detail; however, some results are known for oxygen-reconstructed TiO_2(110) [66, 67], mica (001) [68–70] and KCl(100) [71, 72] surfaces. From STM, LEED and ultraviolet photoelectron spectroscopy (UPS) studies it can be concluded that the first molecular layer is in most cases represented by p-6P molecules which are oriented with the long molecular axes parallel to the substrate surface. However, at elevated temperatures at oxygen-reconstructed TiO_2(110) surfaces a monolayer with up-right standing molecules can be prepared [52, 73].

The growth kinetics of sub-monolayers, monolayers and multilayers is studied by TDS. TDS spectra are recorded from different layer thicknesses, ranging from 0.1 nm up to several nanometres. In the case of Au(111) and mica (001) it could be concluded that the first monolayer is closed at a thickness of about 0.31 and 0.2 nm, respectively. This value corresponds approximately to the van der Waals thickness of a single molecule, therefore it is concluded that the molecules are oriented in the first monolayer with their long molecular axis parallel to the substrate surface. Figure 5 shows TDS spectra of p-6P thin films prepared with a nominal thickness of 0.4 nm on three different single-crystalline surfaces. The desorption features of the first monolayers are clearly visible for films prepared on Au(111) and mica (001) surfaces with peak maxima at 640 and 540 K, respectively [58, 70]. More detailed TDS investigations reveal the desorption energy of a single molecule on the Au(111) surface as 3.6 eV for the monolayer [58]. Thickness-dependent TDS studies reveal the nominal thickness of the first monolayer at 0.31 and 0.2 nm for Au(111) and mica (001), respectively. The desorption feature of p-6P multilayers (layers upon the first monolayer) appears at temperatures between 450 and 500 K. In the case of Au(111), only the onset of the multilayer peak is visible, since

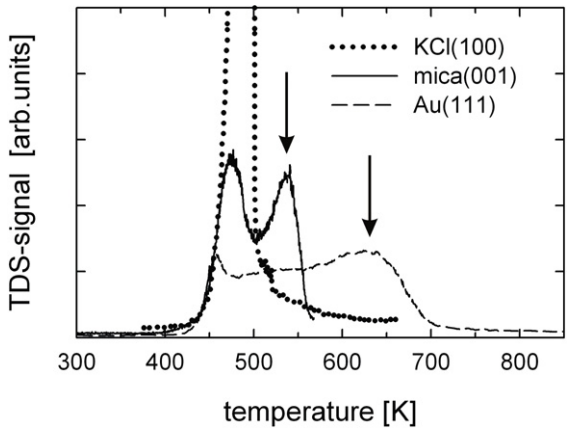

Figure 5. Thermal desorption spectroscopy (TDS) on a sexiphenyl film with a nominal thickness of 0.4 nm prepared on a KCl(100), mica (001) and gold(111) surface. Arrows indicate the desorption temperature of the first saturated monolayer. The data are provided courtesy of A Winkler.

most of the material is already bound in the first monolayer. The multilayer peak is clearly present on the mica (001) surface. The desorption energy of a single molecule from the multilayer is 2.4 eV [58]. In the case of KCl(100), no monolayer desorption is observed, which means that no closed monolayer is formed and the deposited material immediately forms molecular clusters [72]. This is confirmed by AFM studies, since a morphology of extended needles is already present in thin films with a nominal thickness of smaller than 1 nm [74].

From the TDS studies it can be concluded that, for the three surfaces that are compared, the interaction of p-6P molecules with Au(111) is stronger than with mica (001), but in both cases the substrate–molecule interaction exceeds the molecule–molecule interaction. On KCl(100) the intermolecular interactions even exceed the substrate–molecule interaction. As a consequence of the interaction strengths, a wetting layer is formed on Au(111) and mica (001) surfaces and no wetting layer is present on the KCl(100) surface.

The strong interaction strength of p-6P with the Au(111) surface results in crystal growth with orientation D, which reflects the initially *flat-on* oriented molecules. The weaker interaction strength of p-6P with mica (001) results in an increasing importance of the intermolecular interactions which initiate the crystal orientations B and C. Both crystal orientations are formed by alternating *edge-on* and *side-tilted* molecules with the long molecular axes 5° off from the substrate surface.

7. Sexiphenyl thin films on dielectric surfaces

The TDS investigations (figure 5) reveal that the interaction of p-6P with dielectric surfaces like KCl(100) and mica (001) is weaker than with metallic surfaces. This fact implies that on dielectric surfaces the migration of the molecules on the substrate surface is more easily possible and that intermolecular interactions play a more important role in the formation of the first molecular layers. The crystal

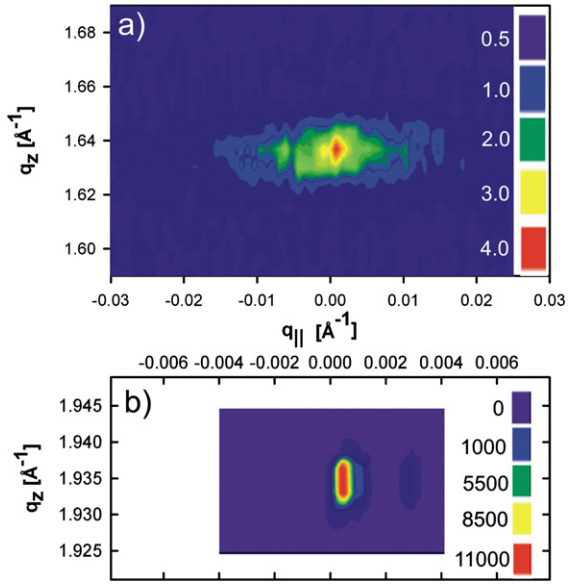

Figure 6. Reciprocal space map of a 30 nm thick sexiphenyl thin film grown on $TiO_2(110)$ substrate measured with a high-resolution laboratory setup. The specular reflection of sexiphenyl (a) and of the substrate (b) are compared. The intensity levels are given in counts/second at the right-hand part of the diagrams.

orientations of p-6P which are grown on dielectric surfaces show orientations A, B, C and S.

P-6P thin films prepared on uniaxially pre-treated surfaces (like a rubbed polymer surface) appear in a morphology with elongated islands [75–77]. The aspect ratio of the islands is influenced by the substrate temperature during the film growth and is found to be below 10 [55]. Depending on the rubbing procedure, different crystal orientations appear. Detailed crystallographic studies on a p-6P film grown on a previously deposited and *ex situ* rubbed p-6P layer reveal a biaxial alignment of p-6P crystallites with orientation A. It is found that the long molecular axes are parallel to the rubbing direction [78].

Elongated islands with aspect ratios larger than 10 (needle-like morphology) are found on thin films grown on oxygen-reconstructed $TiO_2(110)$ surfaces [66]. Thin films with a nominal thickness of 0.3 nm already show a needle-like morphology which is present in thin films up to a thickness of 30 nm. Specular diffraction shows the $20\bar{3}$ reflection, which reveals crystal orientation A. Figure 6 shows a two-dimensional reciprocal space map of a p-6P thin film grown on a $TiO_2(110)$ surface. The specular $20\bar{3}$ reflection of p-6P (figure 6(a)) is mapped and compared with the specular 110 reflection of the substrate (figure 6(b)). The peak widths in q_z direction are comparable with 0.014 and 0.006 Å^{-1} for p-6P ($20\bar{3}$) and $TiO_2(110)$, respectively. However, the rocking width of p-6P is considerably larger than the substrate rocking widths: values of 0.01 and 0.0004 Å^{-1} are observed for p-6P and the substrate, respectively. From the peak width in q_z, the crystal size perpendicular to the substrate surface can be estimated; a value of about 50 nm is obtained. This value seems to be reasonable, since the island-type crystals are expected to be higher than the nominal film thickness of 30 nm. The

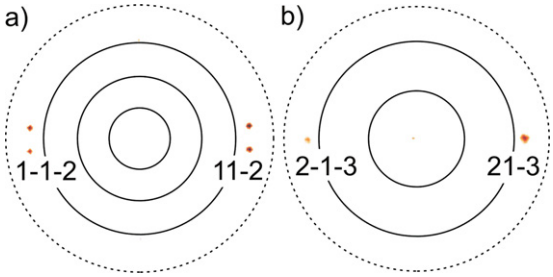

Figure 7. Two selected pole figures of a 30 nm thick film of sexiphenyl grown on a $TiO_2(110)$ surface representing the spatial distribution of the $\{11\bar{2}\}$ reflections (a) and of the $\{21\bar{3}\}$ reflections (b). The circles give the ψ-scale in steps of 15°; the measurement limit is marked with a dotted circle. The enhanced pole densities of only one crystal alignment are indexed.

width in the $q_{||}$ direction is 20 times larger for p-6P than that of the substrate. A reason for that difference can be found in the difference in the lateral crystal size and the mosaicity of the epitaxially grown crystallites.

The epitaxial order (the in-plane order) of p-6P crystallites grown on $TiO_2(110)$ is determined by the x-ray diffraction pole figure technique. Figure 7 shows two selected pole figures taken for $\{11\bar{2}\}$ reflections (figure 5(a)) and for $\{21\bar{3}\}$ reflections (figure 5(b)). The pole figures reveal that two different crystal alignments are present within the film, and the epitaxial relationships and the epitaxial matrices can be determined unambiguously [27]. Both crystal structures have in common that the long molecular axes are aligned along the distinct [001] surface direction of $TiO_2(110)$. A strong surface corrugation determined by rows of oxygen atoms along $[001]_{TiO_2}$ causes the alignment of the molecules [66]. The *side-tilted* orientation of the aromatic planes of p-6P is probably already determined in the first monolayer, since the distance between the oxygen rows (0.65 nm) is slightly smaller than the van der Waals width (0.72 nm) of the molecule.

The early growth stage of p-6P on $TiO_2(110)$ is investigated by in-situ studies using grazing incidence diffraction. Figure 8 shows the development of the $00\underline{13}$ and $0\bar{2}\bar{6}$ diffraction peaks as a function of the film thickness. While $00\underline{13}$ arises from net planes which are parallel to the needle axes, the $0\bar{2}\bar{6}$ plane is approximately perpendicular to the needle axes. It is observed that at a nominal film thickness of 0.6 nm the bulk structure of p-6P is already present and that the peak widths are not affected by the film thickness. From the peak width the crystal size in a particular direction of the pole can be estimated, which is about 40 nm for $00\underline{13}$ and 20 nm for $0\bar{2}\bar{6}$. Comparing this result with the observed morphology, it can be concluded that individual needles are composed of several nanocrystals.

Huge efforts were made on the growth of p-6P on alkali halide surfaces like NaCl(100), KBr(100), KCl(100), NaF(100), and LiF(100) [79–82]. It turns out that the most defined growth morphology is formed on KCl(100). Detailed studies of p-6P thin films on KCl(100) surfaces are performed by several groups [20, 50, 53, 54, 83–85]. The early growth stage is orientation A with elongated needles with a length in the μm range [53, 74]. Films with a nominal thickness

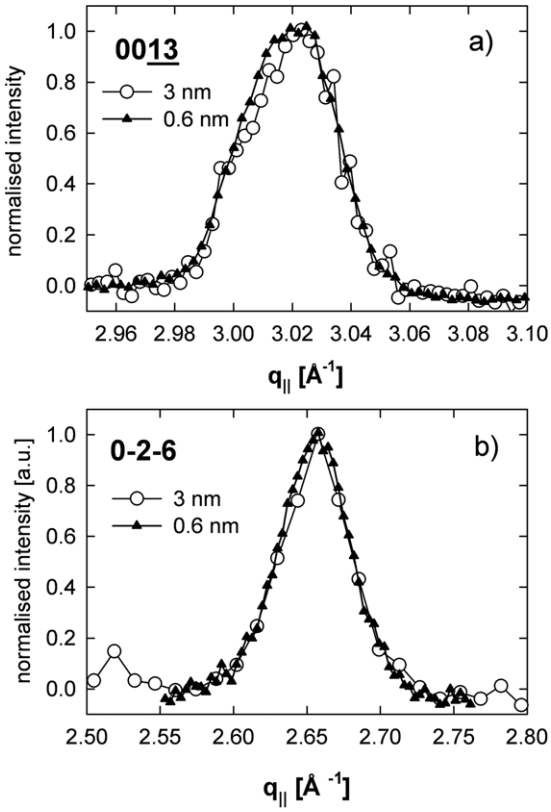

Figure 8. *In situ* grazing incidence diffraction of a sexiphenyl thin film prepared on an oxygen-reconstructed $TiO_2(110)$ surface. The length of the in-plane part of the scattering vector is varied. Two different diffraction peaks are investigated as a function of the film thickness: $00\underline{13}$ (a) and $0\bar{2}\bar{6}$ (b). For presentation, the observed intensities are background subtracted and normalized.

larger than 100 nm show the simultaneous appearance of the four crystal orientations A, B, C and S; all of them are epitaxially ordered [54, 84]. Orientation A, the initial growth orientation, acts as a seed for orientations B and C. A detailed TEM study reveals that the crystal orientations A, B and C show needle-like morphology with different needle widths: orientation B shows thin needles, orientation C thick needles and a medium needle width is found for crystal orientation A [54]. It is shown that the substrate temperature during the thin-film growth favours B and C at low temperatures and orientation S at elevated temperatures [85]. The crystallite size of p-6P needles grown on KCl(100) is investigated by the dark-field method of TEM [50]. It is found that both terraced islands and needles are of single-crystal nature. Needle lengths of up to 10 μm are observed. Deviations from the straight needle morphology are connected with macroscopic crystal defects. In combination with morphology studies on ultra-thin films, it can be concluded that the early growth stage of p-6P needles on KCl(100) already represents extended single crystals which increase in lateral and vertical size during the film growth [74].

A quite different mechanism of the formation of needle-like morphology is observed for p-6P on mica (001). The early growth stage of p-6P on mica yields elongated islands, as shown in figure 4(a). These islands merge together by dynamic coalescence to single needles [69, 86]. The resulting

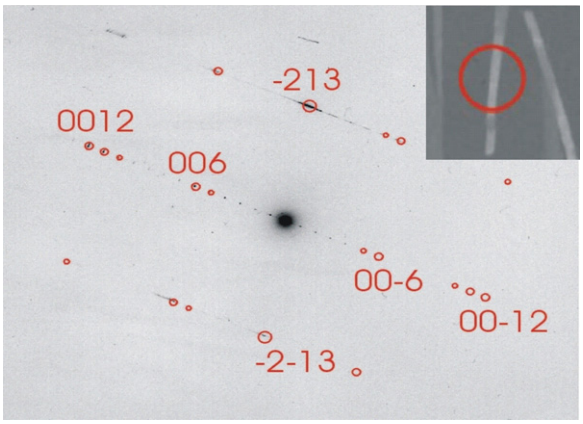

Figure 9. Transmission electron diffraction pattern (and indexation) of a single sexiphenyl needle grown on mica (001). The inset gives—marked by a circle—the individual needle from which the diffraction pattern was taken.

p-6P needles are composed of individual nanocrystals which are connected together by twinning [87]. XRD investigations reveal that p-6P crystals grow on mica (001) surfaces mainly with orientation B; additionally, a minor fraction of orientation C is also observed. Figure 9 shows a transmission electron diffraction (TED) pattern of a single p-6P needle. The inset of figure 9 shows a TEM micrograph of p-6P needles grown on mica (001); a circle marks the individual needle from which the TED pattern is taken. The TED pattern could be indexed on the basis of crystal orientation B. The epitaxial order of orientation B is explained by a two-dimensional lattice match of the hexagonal unit cell of the mica (001) surface with the surface unit cell of the $(11\bar{1})$ net plane defined by the p-6P crystal. A point-on-line coincidence I is observed experimentally and confirmed by lattice mismatch calculations [88, 89].

8. Sexiphenyl thin films on metallic surfaces

The thin-film growth of p-6P on metallic surfaces is determined by the strong interaction of the molecule with the substrate. The structure of the first monolayer is studied on Au(111) and Al(111) surfaces by LEED investigations [58, 62, 63]. By combination of LEED data with XRD results, the alignment of the long molecular axes are determined in the azimuthal direction ($\langle 1\bar{1}0\rangle$) for Al(111) and azimuthal as well as interazimuthal alignments ($\langle 1\bar{1}0\rangle$ and $\langle 11\bar{2}\rangle$) on Au(111) [90, 91]. The orientation of the molecules could be determined as *flat-on* (the aromatic rings parallel to the substrate surface). Please note that the conformation of a single p-6P molecule on metallic surfaces is not flat on average, as it is present in the bulk structure. A distinct tilt angle of neighbouring phenyl rings within a single molecule is observed [61, 62, 92, 93]. Interestingly, the packing of the molecules within the first monolayer is much denser on Al(111) than on Au(111). On Au(111), repulsive interactions between the molecules are responsible for larger intermolecular distances, as is expected from its van der Waals size. In the case of Al(111), a van der Waals-like dense packing of the first monolayer is observed.

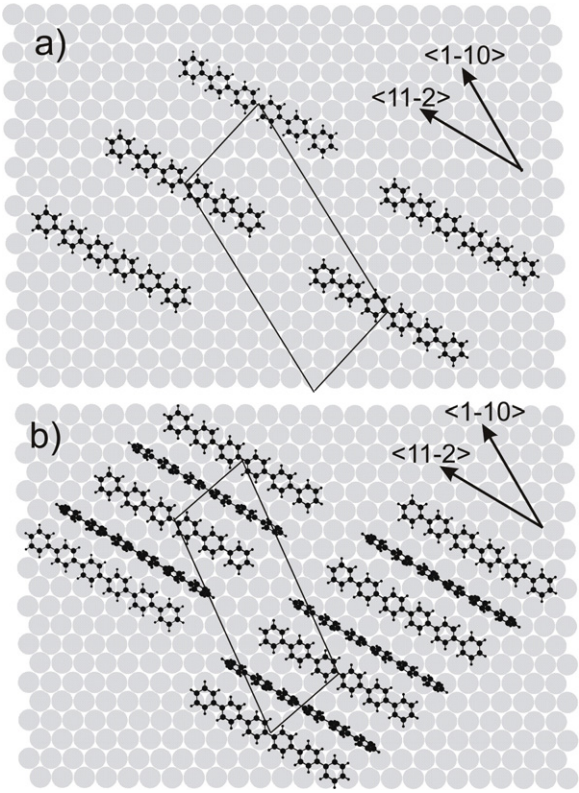

Figure 10. Schematic drawing of the arrangement of the sexiphenyl molecules on a Au(111) surface within the first half monolayer (a) and of the full monolayer (b). The two-dimensional surface unit cells are depicted.

Figure 10 gives a growth model of the first molecular layer on a Au(111) surface, as derived from a combined TDS, NEXAFS, LEED and XRD study. At a nominal layer thickness of 0.25 nm a surface unit cell of $a = 1.4$ nm, $b = 3.4$ nm and $\gamma = 74°$ is found with *flat-on* orientation of the molecules (figure 10(a)). The observed separation of neighbouring molecules of about 1.4 nm is considerably larger than the van der Waals width of a single molecule, which is about 0.72 nm. This separation can be explained by repulsive intermolecular interactions present for aromatic molecules on metallic surfaces [59, 94]. At a nominal film thickness of 0.4 nm a slight change in the surface unit cell is observed (figure 10(b)). It is concluded that the molecules of the second layer are squeezed in an *edge-on* orientation in between the *flat-on* oriented molecules [58, 95]. A similar growth development in the first monolayer was also found for other rod-like aromatic molecules [59, 96].

The epitaxial orientation in thick films (30 nm) was found for p-6P on Au(111) for the crystal orientation D with the long molecular axes either in the $\langle 1\bar{1}0\rangle$ or in the $\langle 11\bar{2}\rangle$ direction of the gold surface. The molecular orientation and alignment in the epitaxially ordered film reflects the molecular order and alignment in the monolayer. Therefore, it can be concluded that the initial order of the molecules determine the epitaxial order.

The arrangement of the molecules within the 0.4 nm thick film on Au(111) shows strong similarities to the packing

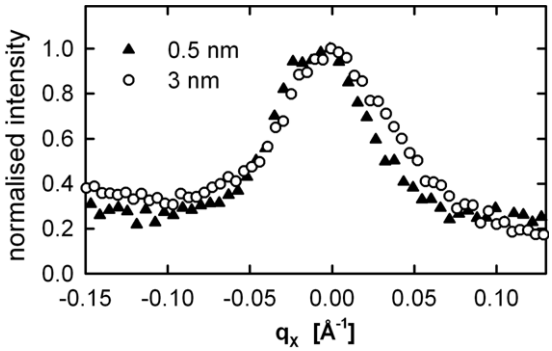

Figure 11. *In situ* grazing incidence x-ray diffraction of a sexiphenyl thin film prepared on an Al(111) surface with two different nominal thicknesses 0.5 and 3 nm. In-plane rocking curves of the $11\bar{1}$ reflections are shown; the intensities are normalized.

of the molecules within the crystal in orientation D. The alternating *flat-on/edge-on* arrangement of the molecules are quite comparable. However, the surface unit cell of the monolayer and of the $(21\bar{3})$ net plane (orientation D) are different. Relaxation of the existing strain between the monolayer lattice and the crystal lattice have to appear. Due to the weak intermolecular interaction, stress within the layer is expected to play a subordinate role but reorientation of the molecules to the bulk structure seems to be present. It can be supposed that the strong interaction of p-6P with Au(111) does not allow a complete re-orientation including the molecules of the monolayer; a discontinuous re-orientation from the monolayer over several molecular layers to the bulk structure can be supposed. The strong adsorption of the molecules in the first monolayer does not allow any re-orientation of the molecule due to the crystallization process. The transition from the monolayer structure to the bulk structure causes mainly lateral distortions which appear in the next layers above the first monolayer.

The appearance of the bulk structure slightly above the monolayer thickness is investigated on Al(111). Figure 11 shows an *in situ* XRD surface diffraction scan (an in-plane rocking curve of the $11\bar{1}$ reflection) on a p-6P thin film grown on Al(111) with different thicknesses. The in-plane peak $11\bar{1}$ (arising from crystal orientation D with aligned molecules along $\langle 1\bar{1}0\rangle_{\mathrm{Al}}$) is already observed at a nominal film thickness of 0.5 nm, which reveals that, at thicknesses slightly larger than the monolayer thickness, the crystal structure of p-6P is developed and that the epitaxial order is already present. It is observed that the peak widths of the 0.5 and 3 nm thick films are the same and that no change with the nominal film thickness is observed. It can be concluded that the in-plane mosaicity is already determined by the alignment of the initial crystallites.

While p-6P films grown at 340 K show a quite perfect molecular alignment along the azimuthal as well as inter-azimuthal directions, a slight difference in the molecular alignment is observed for p-6P on Au(111) when the film is prepared at a substrate temperature of 300 K. The long molecular axes are turned 3° off-axis from the inter-azimuthal surface direction. This fact is explained by a two-dimensional

lattice matching of the $21\bar{3}$ plane of p-6P (crystal orientation D) with the Au(111) surface which encloses a point-on-line coincidence I with each other [91]. This means that, at a substrate temperature of 300 K, the deposition of multilayer films causes a change in the monolayer structure, so that the crystallographic $21\bar{3}$ is formed parallel to the Au(111) surface.

9. Conclusions

The properties of p-6P thin films are studied extensively for applications in organic opto-electronics. Knowledge of tuning the orientation and alignment of p-6P crystals, as well as crystal sizes, is important for successful application. The structural properties of p-6P on different surfaces is studied using surface science methods in the sub-monolayer, in the monolayer and in the multilayer regime; and the results are combined with crystallographic and microscopic investigations on films with a thickness starting from a nominal thickness of 0.5 nm up to 100 nm.

Depending on the type of substrate, different preferred orientations of the crystallites are found; the results are collected in table 1. Pronounced differences are found between dielectric and metallic surfaces. In the case of metallic surfaces, the strong interaction between the p-6P molecule and the substrate surface determines the orientation of the molecules in the first monolayers, which are oriented *flat-on* relative to the substrate surface. The bulk crystal structure is formed at a nominal film thickness of slightly larger than a single monolayer. The (out-of-plane) orientation and the (in-plane) alignment of the molecules remain through the whole film. In the case of dielectric surfaces, the intermolecular interactions have a stronger influence on the formation of the first monolayer, leading to a variety of different crystal orientations appearing on dielectric surfaces. The quality of the surface and surface contamination has a strong influence on the first monolayer and therefore also on the crystal growth of p-6P. Thin films prepared on single-crystalline surfaces at substrate temperatures between room temperature and 470 K are epitaxially ordered.

Acknowledgments

This work was supported by the Austrian Science Fund (FWF) through the National Science Network 'Interface Controlled and Functionalized Organic Films'. The author acknowledges the European Synchrotron Facility for the provision of synchrotron radiation facilities and T Schülli for his assistance in using the beamline BM32. Many thanks to the surface scientists who provided excellent samples for diffraction studies and for stimulating discussions on thin-film growth: Mike Ramsey and Georg Koller, Karl Franzens University Graz, Austria; Adi Winkler, Graz University of Technology, Austria. High-quality samples were also provided by A Andreev and H Sitter, University Linz, Austria. Many thanks to my colleagues for thin-film characterization: A Thierry, Institute Charles Sadron, Strasbourg, France for transmission electron diffraction; A Satka and J Kovac, Laser Center, Bratislava, Slovakia for scanning electron microscopy and C Teichert, Leoben, Austria for atomic force microscopy. Last but not least I have to thank all the PhD and masters students who worked under my supervision on the structural characterization of p-6P thin films: Kurt Erlacher, Harald Plank, Ingo Salzmann, Martin Oehzelt, Ondrej Lengyel, Thomas Haber and Oliver Werzer.

References

[1] Seki K, Karlsson U O, Engelhardt R, Koch E-E and Schmidt W 1984 *Chem. Phys.* **91** 459
[2] Puschnig P and Ambrosch-Draxl C 1999 *Phys. Rev.* B **60** 7891
[3] Graupner W, Meghdadi F, Leising G, Lanzani G, Nisoli M, De Silvestri S, Fischer W and Stelzer F 1997 *Phys. Rev.* B **56** 10128
[4] Stampfl J, Tasch S, Leising G and Scherf U 1995 *Synth. Met.* **71** 2125
[5] Graupner W, Grem G, Meghdadi F, Paar C, Leising G, Scherf U, Müllen K, Fischer W and Stelzer F 1994 *Mol. Cryst. Liq. Cryst.* **256** 549
[6] Leising G, Tasch S, Meghdadi F, Athouel L, Froyer G and Scherf U 1996 *Synth. Met.* **81** 185
[7] Era M, Tsutsui T and Saito S 1995 *Appl. Phys. Lett.* **67** 2436
[8] Ohmori Y, Tsukagawa T and Kajii H 2001 *Displays* **22** 6
[9] Löfken J O 2005 *Physik J.* **4** 16
[10] Yanagi H and Morikawa T 1999 *Appl. Phys. Lett.* **75** 187
[11] Balzer F, Bordo V G, Simonsen A C and Rubahn H-G 2003 *Phys. Rev.* B **67** 115408
[12] Balzer F and Rubahn H-G 2005 *Adv. Funct. Mater.* **15** 17
[13] Jensen C C and Schroder H 1992 *Appl. Opt.* **31** 7012
[14] Seliskar C J, Landis D A, Kauffman J M, Aziz M A, Steppel R N, Kelley C J, Quin Y and Ghiorghis A 1993 *Laser Chem.* **13** 19
[15] Marcy H O, Rosker M J, Warren L F, Reinhardt B A, Sinclair M and Seager C H 1994 *J. Chem. Phys.* **100** 3325
[16] Quochi F, Cordella F, Mura A, Bongiovanni G, Balzer F and Rubahn H 2005 *J. Phys. Chem.* B **109** 21690
[17] Schneider D *et al* 2005 *J. Appl. Phys.* **98** 43104
[18] Niko A, Meghdadi F, Ambrosch-Draxl C, Vogl P and Leising G 1996 *Synth. Met.* **76** 177
[19] Mikami T and Yanagi H 1998 *Appl. Phys. Lett.* **73** 563
[20] Yanagi H and Okamoto S 1997 *Appl. Phys. Lett.* **71** 2563
[21] Resel R, Oehzelt M, Haber T, Hlawacek G, Teichert C, Müllegger S and Winkler A 2005 *J. Cryst. Growth* **283** 397
[22] Winter B, Berkebile S, Ivanco J, Koller G, Netzer F P and Ramsey M G 2006 *Appl. Phys. Lett.* **88** 253111
[23] Müllegger S and Winkler A 2005 *Surf. Sci.* **574** 322
[24] Ivanco J, Haber T, Resel R, Netzer F P and Ramsey M G 2006 *Thin Solid Films* **514** 156
[25] Sitter H, Andreev A, Teichert C, Hlawacek G, Haber T, Smilgies D M, Resel R, Ramil A M and Sariciftci N S 2005 *Phys. Status Solidi* b **242** 1877
[26] Müllegger S, Hlawacek G, Haber T, Frank P, Teichert C, Resel R and Winkler A 2007 *Appl. Phys.* A **87** 103
[27] Haber T and Resel R 2007 Crystallography of ultrathin organic films and nanoaggregates *Organic Nanostructures for Next Generation Devices* (*Springer Series in Material Sciences*) (Berlin: Springer)
[28] Baker K N, Fratini A V, Resch T, Knachel H C, Adams W W, Socci E P and Farmer B L 1993 *Polymer* **34** 1571
[29] Toudic B, Limelette P, Froyer G, Le Gac F, Moreac A and Rabiller P 2005 *Phys. Rev. Lett.* **95** 215502
[30] Smilgies D-M 2005 *Acta Crystallogr.* B **61** 357
[31] Stevens B 1962 *Spectrochim. Acta* **18** 439
[32] Desiraju G R and Gavezzotti A 1989 *Acta Crystallogr.* B **45** 473

[33] Williams D E and Xiao Y 1993 *Acta Crystallogr.* A **49** 1
[34] Klymenko V E and Rozembaum V M 1999 *J. Chem. Phys.* **110** 5978
[35] Nabok D, Puschnig P and Ambrosch-Draxl C 2007 at press
[36] Athouel L, Froyer G and Riou M T 1993 *Synth. Met.* **55–57** 4734
[37] Resel R, Koch N, Meghdadi F, Leising G, Athouel L, Froyer G and Hofer F 2001 *Cryst. Res. Technol.* **36** 47
[38] Resel R, Koch N, Meghdadi F, Leising G, Unzog W and Reichmann K 1997 *Thin Solid Films* **305** 232
[39] Resel R and Leising G 1998 *Surf. Sci.* **409** 302
[40] Gundlach D J, Jackson T N, Schlom D G and Nelson S F 1999 *Appl. Phys. Lett.* **74** 3302
[41] Yoshida H, Inaba K and Sato N 2007 *Appl. Phys. Lett.* **90** 181930
[42] Servet B *et al* 1994 *Chem. Mater.* **6** 1809
[43] Koch N, Resel R, Meghdadi F, Leising G and Reichmann K 1997 *Synth. Met.* **84** 649
[44] Blumstengel S, Meinardi F, Tubino R and Borghesi A 2003 *Synth. Met.* **137** 961
[45] Berkebile S, Koller G, Hlawacek G, Teichert C, Netzer F P and Ramsey M G 2006 *Surf. Sci.* **600** L313
[46] Müller B, Kuhlmann T, Lischka K, Schwer H, Resel R and Leising G 1998 *Surf. Sci.* **418** 256
[47] Andreev A, Matt G, Brabec C J, Sitter H, Badt D, Seyringer H and Sariciftci N S 2000 *Adv. Mater.* **12** 629
[48] Balzer F and Rubahn H-G 2002 *Surf. Sci.* **507–510** 588
[49] Hlawacek G, Teichert C, Andreev A Y, Sitter H, Berkebile S, Koller G, Ramsey M and Resel R 2005 *Phys. Status Solidi* a **202** 2376
[50] Haber T, Oehzelt M, Andreev A, Thierry A, Sitter H, Smilgies D-M, Schaffer B, Grogger W and Resel R 2006 *J. Nanosci. Nanotechnol.* **6** 698
[51] Athouel L, Resel R, Koch N, Meghdadi F, Froyer G and Leising G 1999 *Synth. Met.* **101** 627
[52] Resel R *et al* 2006 *Surf. Sci.* **600** 4645
[53] Haber T, Andreev A, Oehzelt M, Smilgies D-M, Sitter H and Resel R 2007 *Cryst. Growth Des.* submitted
[54] Haber T, Andreev A, Thierry A, Sitter H, Oehzelt M and Resel R 2005 *J. Cryst. Growth* **284** 209
[55] Brandt H-J, Resel R, Keckes J, Koppelhuber-Bitschnau B, Koch N and Leising G 1999 *Mater. Res. Soc. Symp. Proc.* **561** 161
[56] Oehzelt M, Müllegger S, Winkler A, Hlawacek G, Teichert C and Resel R 2004 *Mater. Struct.* **11** 155
[57] France C B and Parkinson B A 2003 *Appl. Phys. Lett.* **82** 1194
[58] Müllegger S and Winkler A 2006 *Surf. Sci.* **600** 1290
[59] Müllegger S, Salzmann I, Resel R, Hlawacek G and Teichert C 2004 *J. Chem. Phys.* **121** 2272
[60] Müllegger S and Winkler A 2005 *Surf. Sci.* **574** 322
[61] Koller G, Surnev S, Ramsey M G and Netzer F P 2004 *Surf. Sci.* **559** L187
[62] Winter B, Ivanco J, Salzmann I, Resel R, Netzer F P and Ramsey M G 2004 *Langumir* **20** 7512
[63] Winter B, Ivanco J, Netzer F P and Ramsey M G 2003 *Thin Solid Films* **433** 269
[64] Hu Y, Maschek K, Sun L D, Hohage M and Zeppenfeld P 2006 *Surf. Sci.* **600** 762
[65] Oehzelt M, Grill L, Berkebile S, Koller G, Netzer F P and Ramsey M G 2007 *Chem. Phys. Chem.* **8** 1707
[66] Koller G, Berkebile S, Krenn J R, Tzvetkov G, Hlawacek G, Lengyel O, Netzer F P, Teichert C, Resel R and Ramsey M 2004 *Adv. Mater.* **16** 2159
[67] Sun L D, Hohage M, Zeppenfeld P, Berkebile S, Koller G, Netzer F P and Ramsey M G 2006 *Appl. Phys. Lett.* **88** 121913
[68] Balzer F and Rubahn H-G 2001 *Appl. Phys. Lett.* **79** 3860
[69] Teichert C, Hlawacek G, Andreev A Y, Sitter H, Frank P, Winkler A and Sariciftci S 2006 *Appl. Phys.* A **82** 665
[70] Frank P, Hlawacek G, Lengyel O, Satka A, Teichert C, Resel R and Winkler A 2007 *Surf. Sci.* **601** 2152
[71] Balzer F and Rubahn H-G 2004 *Surf. Sci.* **548** 170
[72] Frank P, Hernandez-Sosa G, Sitter H and Winkler A 2007 *Thin Solid Films* at press
[73] Sun L, Berkebile S, Koller G, Hohage M, Netzer F P, Zeppenfeld P and Ramsey M G 2007 *Surf. Sci. Lett.* submitted
[74] Andreev A, Haber T, Smilgies D-M, Resel R, Sitter H, Sariciftci N S and Valek L 2005 *J. Cryst. Growth* **275** e2037
[75] Yase K, Han E M, Yamamoto K, Yoshida Y, Takada N and Tanigaki N 1997 *Japan. J. Appl. Phys.* **36** 2843
[76] Hu W-S, Lin Y-F, Tao Y-T, Hsu Y-J and Wei D-H 2005 *Macromolecules* **38** 9617
[77] Aoki N, Koshiba Y and Ueda Y 2005 *Japan. J. Appl. Phys.* **44** 4088
[78] Erlacher K, Resel R, Keckes J, Meghdadi F and Leising G 1999 *J. Cryst. Growth* **206** 135
[79] Andreev A and Sitter H 2002 private communications
[80] Kintzel E J, Smilgies D-M, Skofronick J G, Safron S A and Van Winkle D H 2006 *J. Cryst. Growth* **289** 345
[81] Yoshida Y, Takiguchi H, Hanada T, Tanigaki N, Han E M and Yase K 1998 *Appl. Surf. Sci.* **130–132** 651
[82] Balzer F and Rubahn H-G 2001 *Proc. SPIE* **446** 238
[83] Kawaguchi A, Tsuji M, Moriguchi S, Uemura A, Isoda S, Ohara M, Petermann J and Katayama K 1986 *Bull. Inst. Chem. Res. Kyoto Univ.* **64** 54
[84] Smilgies D-M, Boudet N and Yanagi H 2002 *Appl. Surf. Sci.* **189** 24
[85] Kintzel E J, Smilgies D-M, Skofronick J G, Safron S A and Van Winkle D H 2004 *J. Vac. Sci. Technol.* A **22** 107
[86] Andreev A, Sitter H, Brabec C J, Hinterdorfer P, Springholz G and Sariciftci N S 2001 *Synth. Met.* **121** 1379
[87] Plank H, Resel R, Sitter H, Andreev A, Sariciftci N S, Hlawacek G, Teichert C, Thierry A and Lotz B 2003 *Thin Solid Films* **443** 108
[88] Hooks D E, Fritz T and Ward M D 2001 *Adv. Mater.* **13** 227
[89] Resel R, Haber T, Balzer F and Rubahn H G 2007 in preparation
[90] Resel R, Salzmann I, Hlawacek G, Teichert C, Koppelhuber B, Winter B, Krenn J K, Ivanco J and Ramsey M G 2004 *Org. Electron.* **5** 45
[91] Haber T, Müllegger S, Winkler A and Resel R 2006 *Phys. Rev.* B **74** 045419
[92] Hla S W, Braun K F, Wassermann B and Rieder K-H 2004 *Phys. Rev. Lett.* **93** 208302
[93] Braun K F and Hla S W 2005 *Nano Lett.* **5** 73
[94] Rosei F, Schunack M, Naitoh Y, Jiang P, Gourdon A, Laegsgaard E, Stensgaard I, Joachim C and Besenbacher F 2003 *Prog. Surf. Sci.* **71** 95
[95] Müllegger S, Hänel K, Strunskus T, Wöll C and Winkler A 2006 *Chem. Phys. Chem.* **7** 2552
[96] Franke R, Franke S, Wagner C, Dienel T, Fritz T and Mannsfeld S C B 2006 *Appl. Phys. Lett.* **88** 161907
[97] Zojer E *et al* 2000 *Phys. Rev.* B **61** 16538
[98] Resel R, Graupner W, Hochfilzer C, Koch N, Meghdadi F, Tasch S, Wohlgenannt M, Leising G and Reichmann K 1998 *Proc. XVII Conf. Appl. Cryst.* (Singapore: World Scientific) p 413
[99] Plank H, Resel R, Purger S, Keckes J, Thierry A, Lotz B, Andreev A, Sariciftci N S and Sitter H 2001 *Phys. Rev.* B **64** 235423
[100] Lengyel O, Satka A, Haber T, Kovac J, Sitter H and Resel R 2007 *Cryst. Res. Technol.* at press